

PAPER

Accurate thickness measurement of graphene

To cite this article: Cameron J Shearer *et al* 2016 *Nanotechnology* **27** 125704

View the [article online](#) for updates and enhancements.

You may also like

- [Biocompatible Exfoliation and Modified Self-Assembly Deposition of Graphene Films for Electrodes Fabrication: Processing Parameters Vs. Electrochemical Performance](#)
Claudio Marchi, Harrison Loh, Luca Magagnin *et al.*
- [High-speed digitization of the amplitude and frequency in open-loop sideband frequency-modulation Kelvin probe force microscopy](#)
Gheorghe Stan
- [Stacked graphene with nanoscale wrinkles supports osteogenic differentiation of human adipose-derived stromal cells](#)
Jong Bo Park, Ji Yeon Ahn, Woo Sub Yang *et al.*



PRIME
PACIFIC RIM MEETING
ON ELECTROCHEMICAL
AND SOLID STATE SCIENCE

HONOLULU, HI
Oct 6–11, 2024

Abstract submission deadline:
April 12, 2024

Learn more and submit!



Joint Meeting of

The Electrochemical Society
•
The Electrochemical Society of Japan
•
Korea Electrochemical Society

Accurate thickness measurement of graphene

Cameron J Shearer, Ashley D Slattery, Andrew J Stapleton,
Joseph G Shapter and Christopher T Gibson

Centre for NanoScale Science and Technology, School of Chemical and Physical Sciences, Flinders University, Bedford Park, South Australia, 5042, Australia

E-mail: cameron.shearer@flinders.edu.au and christopher.gibson@flinders.edu.au

Received 17 November 2015, revised 11 January 2016


Accepted for publication 14 January 2016

Published 18 February 2016



Abstract

Graphene has emerged as a material with a vast variety of applications. The electronic, optical and mechanical properties of graphene are strongly influenced by the number of layers present in a sample. As a result, the dimensional characterization of graphene films is crucial, especially with the continued development of new synthesis methods and applications. A number of techniques exist to determine the thickness of graphene films including optical contrast, Raman scattering and scanning probe microscopy techniques. Atomic force microscopy (AFM), in particular, is used extensively since it provides three-dimensional images that enable the measurement of the lateral dimensions of graphene films as well as the thickness, and by extension the number of layers present. However, in the literature AFM has proven to be inaccurate with a wide range of measured values for single layer graphene thickness reported (between 0.4 and 1.7 nm). This discrepancy has been attributed to tip-surface interactions, image feedback settings and surface chemistry. In this work, we use standard and carbon nanotube modified AFM probes and a relatively new AFM imaging mode known as PeakForce tapping mode to establish a protocol that will allow users to accurately determine the thickness of graphene films. In particular, the error in measuring the first layer is reduced from 0.1–1.3 nm to 0.1–0.3 nm. Furthermore, in the process we establish that the graphene-substrate adsorbate layer and imaging force, in particular the pressure the tip exerts on the surface, are crucial components in the accurate measurement of graphene using AFM. These findings can be applied to other 2D materials.

 Online supplementary data available from stacks.iop.org/NANO/27/125704/mmedia

Keywords: graphene, atomic force microscopy, graphite

(Some figures may appear in colour only in the online journal)

1. Introduction

Graphene is an atomic layer of sp^2 hybridized carbon which exhibits remarkable electronic, optical and mechanical properties [1–3]. These properties have been found to vary, often significantly, with the number of graphene layers (N) present in a sample and with the presence of defects in the sp^2 structure [2, 4–8]. Consequently, the accurate and reliable determination of graphene layer number in a sample is vital for determining structure–property relationships.

Graphene layer number can be approximated using optical techniques such as Rayleigh imaging and Raman spectroscopy [9, 10]. Rayleigh imaging relies on interferometric contrast between graphene and the underlying substrate upon white light illumination. The resulting contrast can rapidly give information on the thickness of graphene but is limited to particular substrates (e.g. 300 nm SiO_2/Si) and cannot accurately determine layer number, particularly for $N > 6$ [9]. Raman spectroscopy has proven to be the technique of choice for determining N since particular features of

the Raman spectrum are highly dependent upon N . The most prominent changes occur to the 2D band ($\sim 2600\text{--}2700\text{ cm}^{-1}$) which broadens and alters in shape, and changes position and intensity with $1 \leq N \leq 10$ [11]. More recently, the interlayer shear peak (C-peak, $\sim 30\text{--}45\text{ cm}^{-1}$) has also been shown to increase in intensity and position with $2 \leq N \leq 8$ [12]. In practise, by comparing an obtained Raman spectrum of an unknown graphene sample to that of one of many literature spectra, N can be approximated [13]. However, Raman spectroscopy is limited to high quality graphene with very few structural/chemical defects, and is much more reliable for few layer ($N < 4$) samples than for thicker samples which are generally much more common (depending on synthesis technique).

With the inherent limitations of optical characterization, researchers are searching for a universal technique which is capable of accurately determining N for all N , regardless of structural defects and substrate. Scanning probe microscopy techniques, such as atomic force microscopy (AFM), are commonly used to accurately determine the thickness of nanomaterials. In fact, the first reported isolation of graphene was confirmed via AFM [14]. However, careful inspection of the current literature reveals that AFM has been an inaccurate and unreliable method for N determination, particularly for single layer graphene (SLG) with reported values of thickness in the literature ranging from 0.4 to 1.7 nm (table 1) which varies widely when compared to the inter-plane spacing of graphite (0.335 nm) [15]. The variation is generally regarded to be related to variations in interactions such as substrate-graphene and AFM probe-graphene which depend upon substrate surface energy, graphene structure and sample preparation. For example, when prepared in a high humidity environment water adlayers have been observed between mica and graphene [16, 17].

Despite the disparity in measured SLG thickness via AFM, it is common to use the following equation to determine N via AFM [13]:

$$N = \frac{(t_{\text{measured}} - 0.4)}{0.335}, \quad (1)$$

where t_{measured} is the measured thickness via AFM and the nominal 0.4 value is subtracted to account for increases in measured thickness related to substrate-graphene and graphene-tip interactions. The value of 0.4 is arbitrary and, according to table 1, can be inaccurate by up to 1 nm (equivalent to three graphene layers assuming a 0.335 nm spacing). When considering the substantial variation in graphene properties with N , improving the accuracy of SLG thickness measured by AFM is required.

One option that has been explored has been optimizing the free amplitude of oscillation in tapping mode (TM) AFM such that the effect of nanomaterial-tip interactions can be effectively negated [18, 19]. When applied to the imaging of graphene, changes to the free amplitude have resulted in measured SLG thickness from 0.4–1.7 nm [20]. The process to determine the optimal free amplitude and imaging set-point is somewhat time consuming and laborious. This optimization of TM also requires the acquisition of amplitude versus

distance curves which can result in tip damage, especially considering TM probes have relatively high spring constants (on the order of $5\text{--}50\text{ N m}^{-1}$) and small radii (typically less than 10 nm). Furthermore, it does not take into account substrate-graphene interactions which are likely to be a greater source of inaccuracy. Calculating the exact imaging force in TM is also more complicated than other imaging modes and therefore reproducibility of results can be difficult [21].

Contact mode AFM has also been used to determine the number of layers of graphene films but differences in height have been observed between forward and reverse scans [20]. These differences have been attributed to the high lateral forces, typical of contact mode, which can result in inaccurate estimation of N .

PeakForce tapping (PFT) is an imaging mode which involves intermittent surface contact up to a set applied force at an oscillation frequency of 0.5–8 kHz. The mode allows the simultaneous measurement of interaction force, adhesion and topography. The peak repulsive interaction force is measured in real-time and is used as the feedback signal, this significantly reduces the effects of common artefacts observed with other AFM techniques, which are associated with forces such as tip-sample adhesion. Here we investigate the effect of applied force and AFM tip geometry on the measured height of graphene samples and use the results to create an accurate, universal method for N determination in graphene samples regardless of defects.

2. Experimental

2.1. Sample preparation and optical characterization

Graphene samples were prepared from the mechanical exfoliation of graphite onto a silicon wafer with 100 nm thermal oxide (CZ, 1–20 $\Omega\text{ cm}$, $\langle 100 \rangle$, ABC GmbH, Germany). The SLG sections/areas on the Si wafer were then identified using the optical microscope on a confocal Raman spectrophotometer (Witec Alpha 300RS 100x, 0.9 numerical aperture, working distance 0.23 mm) to find areas of very thin graphite. Raman single spectra were acquired with a 532 nm YAG laser with tuneable power and collected with integration times of 10 s and three accumulations. Presented single spectra are normalized to the intensity of the G-band. Raman spectral images were obtained by collecting a series of 50×50 single spectra (1.5 s integration per spectrum) over an area of $15 \times 15\text{ }\mu\text{m}$. The plot of the 2D/G band ratio was generated by exporting the values for maximum intensity for the 2D and G bands after using background subtraction (Witec Project 2.1), then computing the value for 2D/G for each position and plotting as a 3D surface matrix (Origin Pro 9.0).

2.2. Scanning probe microscopy

AFM was performed using a Bruker Dimension FastScan AFM with Nanoscope V controller, operating in PFT mode with the humidity controlled, in the immediate vicinity of the instrument, to less than 35% using dehumidifying units (CLI-

Table 1. Summary of selected results for measured single layer graphene thickness measured by AFM with preparation method, AFM method, substrate and whether SLG was confirmed by Raman spectroscopy.

Measured thickness (nm)	Reported no. of layers	Preparation method	SPM method	Substrate	SLG confirmed by Raman?	Notes	Reference
0.9 ± 0.2	1	Mechanical exfoliation	AC ^a -AFM	Si/SiO ₂	Y		[22]
0.4	1	Mechanical exfoliation	UHV ^b NC ^c -AFM	Si/SiO ₂ (300 nm)	N	0.9 nm measured at ambient pressure	[23]
0.4–0.9	1	Mechanical exfoliation	TM ^d -AFM	Mica	Y		[24, 25]
0.4–1.7	1	Mechanical exfoliation	TM-AFM	Si/SiO ₂	Y	Measured SLG height dependant on Free amplitude of cantilever oscillation	[20]
0.9	1	Mechanical exfoliation	Contact-AFM	Si/SiO ₂	N		[14]
0.4–1	1	Mechanical exfoliation	Contact-AFM	Si/SiO ₂	N	First report of AFM of SLG	[26]
1.19 ± 0.1	1	Mechanical exfoliation	IC ^a -AFM	Si/SiO ₂ (300 nm)	Y	Samples were laser irradiated to remove surface adsorbates	[27]
0.7	1	Mechanical exfoliation	Contact-AFM	Si/SiO ₂ (300 nm)	Y		[28]
1	1	Mechanical exfoliation	Contact-AFM	Si(111)	Y		[29]
1.8	1	CVD	TM-AFM	Si/SiO ₂	Y		[30]
1.44	1	RGO	TM-AFM	HOPG	N	AFM able to fold graphene	[31]
0.8–1.5	1	RGO	TM-AFM	Si/SiO ₂ (300 nm)	N	Contact AFM used to remove surface adsorbates	[32]
1.1 ± 0.1	1	GO and RGO	TM-AFM	HOPG	N		[33]
0.9–1.7	1	GO and RGO	TM and Contact AFM	HOPG	N	Height found to depend on AFM imaging mode	[34]
0.8–1.1	1	GO	TM-AFM	Si/SiO ₂ (300 nm)	N	Height changed with GO dispersing solvent	[35]

^a IC and AC = intermittent contact mode.^b UHV = ultra high vacuum.^c NC = non-contact mode.^d TM = tapping mode.

MATE™ model DH2500E). Images were acquired using ScanAsyst-air probes (silicon tips on silicon nitride lever, Bruker) at a scan rate of 1 Hz at a resolution of 512 pixels and 512 lines. The nominal spring constant of the cantilevers is 0.4 N m^{-1} but the true value was determined experimentally prior to each scan using established calibration techniques [36, 37]. The value for PeakForce set point was set prior to capturing an image and calculated by the software using the measured deflection sensitivity and calibrated cantilever spring constant. During a scan topography, adhesion, deformation and hardness were all captured concurrently. Presented AFM topography images have been flattened and analysed using either the depth or step analysis features of Nanoscope Analysis 1.4. Single walled carbon nanotube (SWCNT) modified AFM probes were prepared following a previously reported procedure [38]. More detail is available in the supplementary information.

3. Results and discussion

Graphene samples were prepared by the mechanical exfoliation of graphite onto SiO_2/Si . Optical microscopy was used to find thin graphite flakes which were then analysed via Raman Spectroscopy to determine N . Figure 1(a) shows an 100x objective optical microscope image of a thin graphite flake. The inset of figure 1(a) shows a digital zoom of the area with four circles which correspond with the four areas of the Raman spectra (with matching colour) in figure 1(b). From the position of the 2D band and the relative intensity between the G and 2D band, areas of single-, double-, few- ($N = 3\text{--}5$) and multi- ($N > 5$) layer were found as indicated on figure 1(b) [11, 13]. Raman spectral images of the area were created by taking a series of spectra (50×50) in a raster manner over a $15 \times 15 \mu\text{m}$ area and creating an image from the obtained spectra by plotting the intensity of a selected region of each spectra as a function of XY position. Figure 1(c) represents the intensity of the G-band which correlates with the optical image. Figure 1(d) was obtained by dividing the 2D-band intensity by the G-band intensity to highlight areas of SLG since SLG is expected to have a 2D/G ratio of greater than 2 [10]. SLG areas are observed around the edges of the flake with a large SLG flake found and highlighted in the green box in figure 1(d). AFM of the graphite flake (figures 1(e) and (f)) supports the Raman data and the SLG area shown in figure 1(f) will be used as the main area for subsequent investigation. Interestingly, when imaging with default settings for PFT mode, cross section analysis of SLG shows a measured height of 1.2 nm which is much greater than the theoretical value of 0.335 nm, a commonly observed anomaly (see table 1). This also demonstrates that PFT is not immune from the type of height discrepancies reported for other AFM imaging modes. A significant advantage of PFT mode however is the relative ease in which precise imaging force can be adjusted combined with vastly reduced lateral imaging forces. After obtaining an ideal SLG area, further experimentation was completed to determine if it were possible to accurately measure SLG height.

3.1. Effect of force on graphene height measurement

Several controls were employed to ensure that AFM experiments repeated over multiple days were comparable and that environmental and sample changes were negligible. Prior to AFM, adsorbates were removed from the sample by cleaning with a laser (532 nm) by repeated raster scanning of the graphite flake for 30 min [32, 39]. Raman spectra were collected concurrently with cleaning and indicated that no damage to the graphene occurred, in contrast to a previous report [27], likely due to lesser laser power irradiation and duration. Environmental controls ensured the humidity was less than 35% and the AFM experiments were performed within an acoustic isolation chamber. A new ScanAsyst-air probe was used each session and its spring constant and deflection sensitivity calibrated using established methods before each image was acquired to ensure the applied force remained accurate [36].

PFT AFM of SLG was performed with different peak force set points and AFM images and corresponding measured depth histograms are presented in figure 2. All images have the same z-scale and show how the measured height changes with applied force. Depth plots were obtained from Nanoscope analysis software and show measured heights across the entire image, obtaining heights in this manner is much more accurate and representative of the sample than single cross sections. By fitting two Gaussian functions to the raw data, representing the height of the substrate and SLG, the relative height of SLG could be obtained. With increasing force (figure 2(a)) from 1 to 10 nN the measured height of SLG decreases from 1.69 to 0.43 nm. The change in height is reversible with measured heights from 10 to 1 nN increasing from 0.43 to 1.53 nm (figure 2(b)). The scatter plot of measured height versus force in figure 2(c) suggests a linear correlation. With higher applied force, the measured height approaches that of the true value of 0.335 nm. Due to the roughness of the underlying substrate, the precision in determination of the height becomes low since the fitted Gaussian functions begin to overlap. Flatter substrates such as mica could be used to overcome this limitation but will render it much more difficult to find SLG optically [40]. Nevertheless, the measured height value of 0.43 nm is significantly more accurate than that at lower applied force and represents one of the most accurate values for SLG height determined by AFM (table 1). The trend of decreasing height with increasing force is repeatable and has been measured on multiple occasions with multiple probes (see figures S1 and S2). A linear trend is always observed but the slope varies with AFM probe, indicating that the tip dimension affects the rate of change of the measured height with increasing applied force. With repeating the experiment, it was found that cleaning the sample (completed by scanning with a 532 nm laser) prior to imaging was vital to the regularity of the effect of applied force. The laser cleaning is expected to remove adsorbed organic contaminants which may affect the sample-tip interaction and hence the measured height.

The findings of figures 2, S1 and S2 present two intriguing results that required further investigation. Namely, to

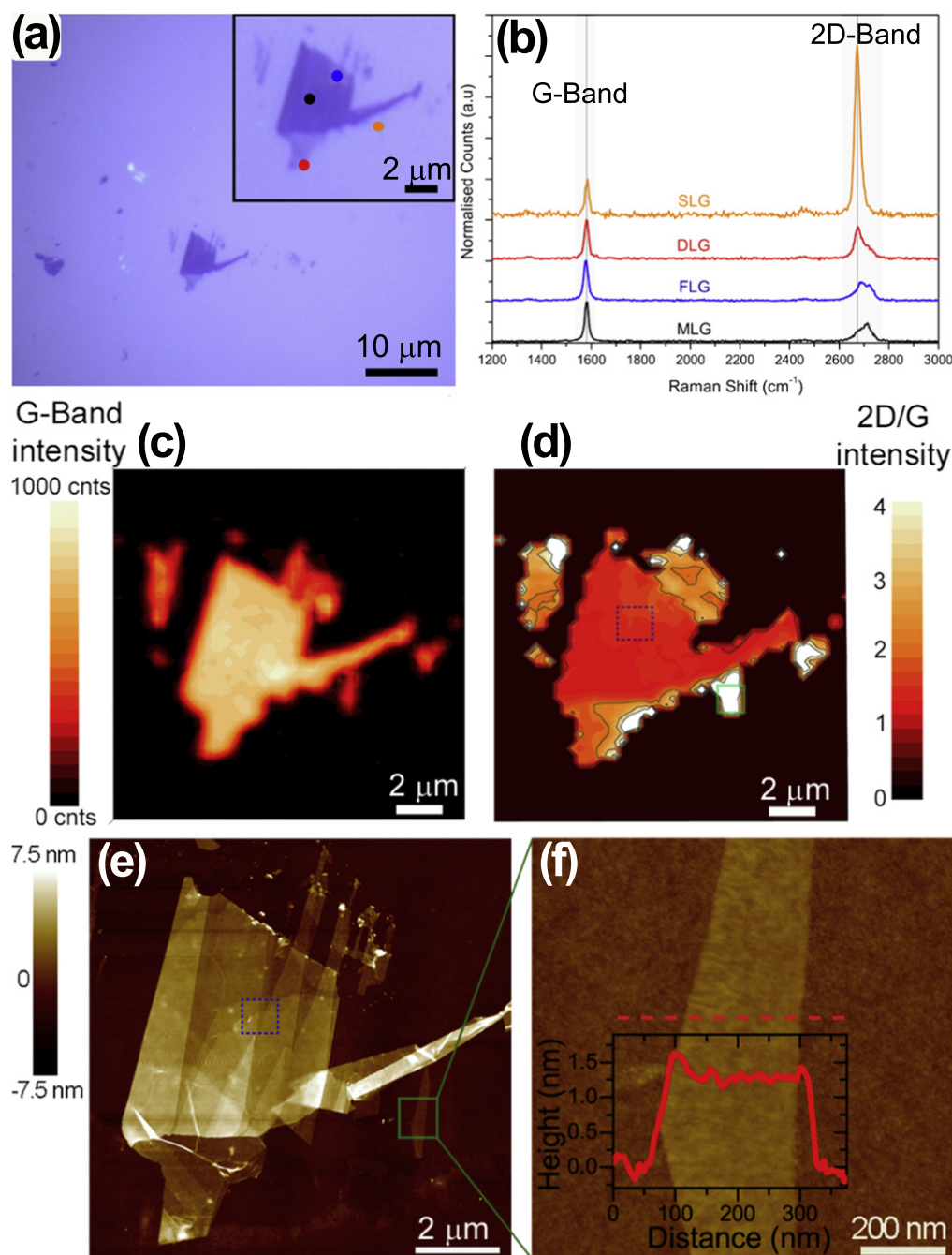


Figure 1. Process used for confirmation of single layer graphene showing (a) optical microscope image (x100) with (inset) digital zoom of graphite flake used for further investigation. (b) Raman spectra of the points highlighted in the inset of (a) corresponding to colour. (c) and (d) Raman spectral images of the graphite flake showing (c) G-band intensity and (d) 2D/G intensity ratio for the area investigated. (e), (f) AFM images of (e) the entire graphite flake and (f) higher magnification AFM image of the single layer area with (inset) cross section graph. SLG area is highlighted in green used for subsequent imaging of SLG. MLG area highlighted in blue is used for MLG imaging.

determine the cause of the overestimation of SLG height at low applied force and the mechanism behind the measured height with different probes changing with force at different rates.

The measured height from AFM is dependent upon a number of interactions including tip-sample, sample-substrate and tip-substrate. To negate the effects of different interactions between tip-graphene and tip-SiO₂ simultaneous adhesion mapping was obtained with topography (an advantage of

the PFT technique). Online supplementary figure S3 displays the adhesion maps obtained simultaneously with the topography images in figure 2(b). The graphene areas show a slightly higher adhesion than the substrate but the magnitude of the adhesion difference between graphene and SiO₂ does not change significantly with applied force (0.1–0.3 nN), suggesting that changes to the adhesion are not responsible for the observed change to height. Furthermore, since the variation in adhesion appears random and does not correlate

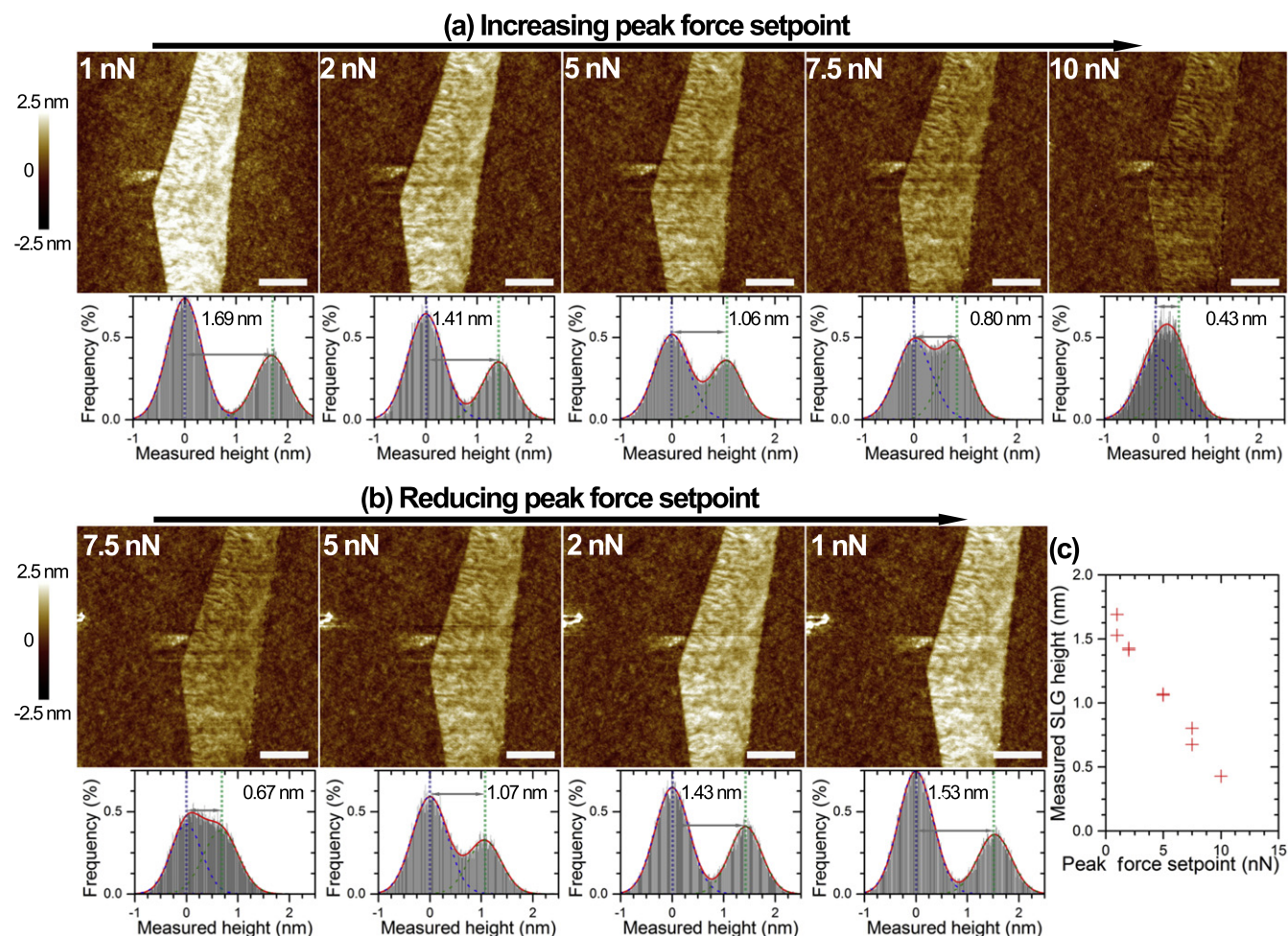


Figure 2. PeakForce tapping mode AFM topography images of graphene showing the change in measured height with peak force set point (as indicated in each AFM image). Images were obtained sequentially by first (a) increasing the peak force set point from 1, 2, 5, 7.5, 10 nN followed by (b) reducing the peak force set point from 7.5, 5, 2, 1 nN. Below each AFM image is the corresponding histogram depth plot from which the graphene height was determined. Scale bar = 200 nm. (c) Graph of measured SLG height versus peak force set point. Images obtained with new ScanAsyst-air probe.

to the force set point, it is interpreted that tip-graphene and tip-substrate interactions remain pseudo constant [31].

The likely cause of the overestimation of graphene height by AFM is adlayers between graphene and the substrate creating a buffer between graphene and substrate. These adlayers have been observed previously [25, 26], but to confirm this, and to ensure that there is not an artefact related to the PFT imaging mechanism at high applied force, the experiment was completed for graphite samples where the underlying substrate is graphite and no adlayer is present. Two samples were investigated: freshly cleaved HOPG (see online supplementary figure S4) and a multi-layer area of the graphite flake (MLG) (black circle in figure 1(a), inset and blue box in figure 1(e)). AFM of MLG steps with increasing applied force are presented in figure 3 where the average step size remains constant at 0.3 ± 0.03 nm. Here, step-analysis was used to average three distinct terraces of the MLG area investigated and the value corresponds very closely to the theoretical height of a single graphene terrace. The same result was obtained for HOPG (online supplementary figure S4). These results show that PFT is capable of accurately

measuring graphene height, regardless of applied force when there is no buffer layer between graphene and substrate. Since the surface energy of MLG and HOPG is analogous to that of SLG [41], tip-substrate and tip-graphene interactions can be negated as being responsible for the overestimation of measured height for SLG samples.

Figures 2 and 3 suggest it is possible to accurately measure graphene height if either (1) high applied force with PFT is used or (2) no buffer layer is present between substrate and graphene. To avoid the inclusion of buffer layers between substrate and graphene, the sample can be prepared in a water free environment such as a nitrogen glove box or under vacuum [29, 39, 40]. However, actually achieving this in practise is, at least, very difficult and often not possible. An easier approach would be to image using PFT with high force to achieve an accurate height measurement. However, imaging with high force will blunt the AFM tip and reduce its lifetime. To work around this limitation, further understanding of why increasing force leads to more accurate measurement was required.

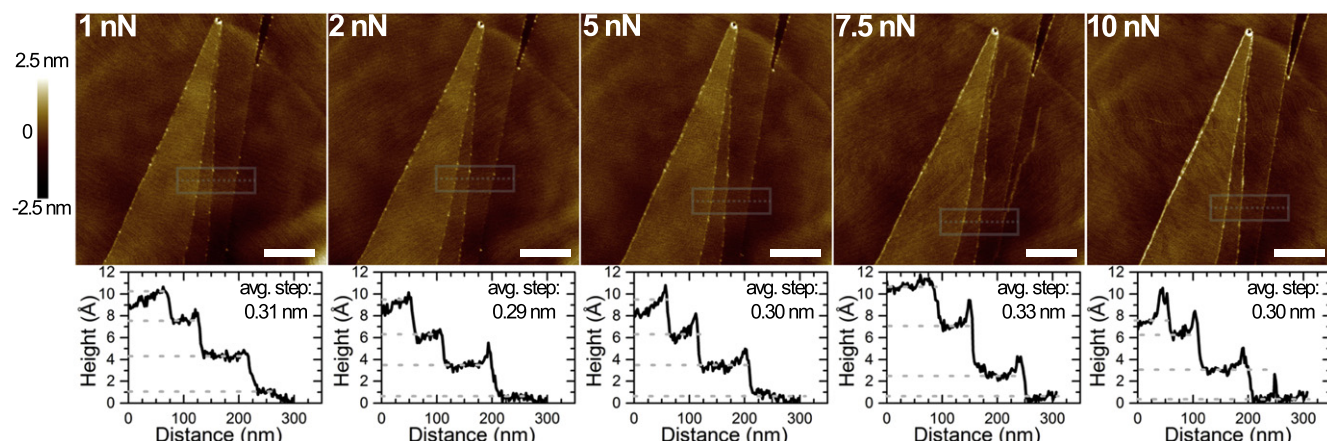


Figure 3. PeakForce tapping mode AFM topography images of multilayer graphene showing the change in measured height with peak force set point (as indicated in each AFM image). Images were obtained sequentially from 1 nN up to 10 nN. Below each AFM image is the corresponding step height plot from which the average graphene step height was determined. Scale bar = 200 nm, grey boxes indicate area where step-height was determined.

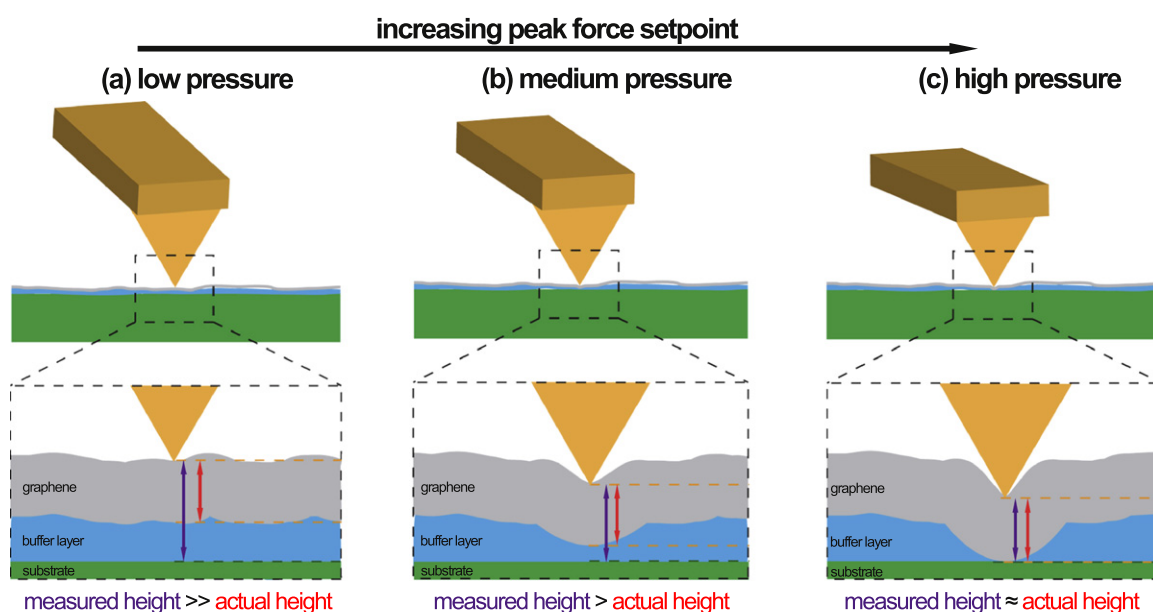


Figure 4. Schematic of proposed mechanism of improving AFM imaging accuracy with increasing peak force set point. As the pressure applied increases from (a) low to (b) medium to (c) high the AFM tip is able to disrupt the underlying buffer layer and subsequently measure a more accurate value for graphene height.

We hypothesize that the key parameter for accurate determination of graphene thickness is the applied pressure. As represented schematically in figure 4, when imaging with low applied pressure (figure 4(a)), the tip lightly presses into the graphene and the measured height is a combination of the thickness of the buffer layer and the graphene. By applying more pressure (figure 4(b)), the tip presses into the graphene and forces it into the buffer layer, reducing the measured height but still measuring a height greater than the actual thickness of graphene. Finally, when applying a high pressure (figure 4(c)), the tip presses the graphene through the entire buffer layer and onto the underlying substrate and measures a height approximately equal to the true thickness of graphene.

3.2. Imaging of graphene with CNT modified AFM probe

To test our hypothesis outlined in figure 4, we repeated our height measurements of SLG with different applied force using an AFM tip with much smaller dimensions. Since pressure is equal to N m^{-2} , it was expected that a lesser force would be required to accurately measure graphene height. Smaller dimension AFM tips were made by placing SWCNTs at the tip apex using a micromanipulator and electron beam processes [38].

PFT imaging of SLG with the sharper SWCNT modified probes with various peak force set points are shown in figure 5(a). Similar to standard probes (figure 2(c)), a linear decrease in measured height was found to occur with increasing applied force from 1.02 nm at 0.5 nN to 0.53 nm at

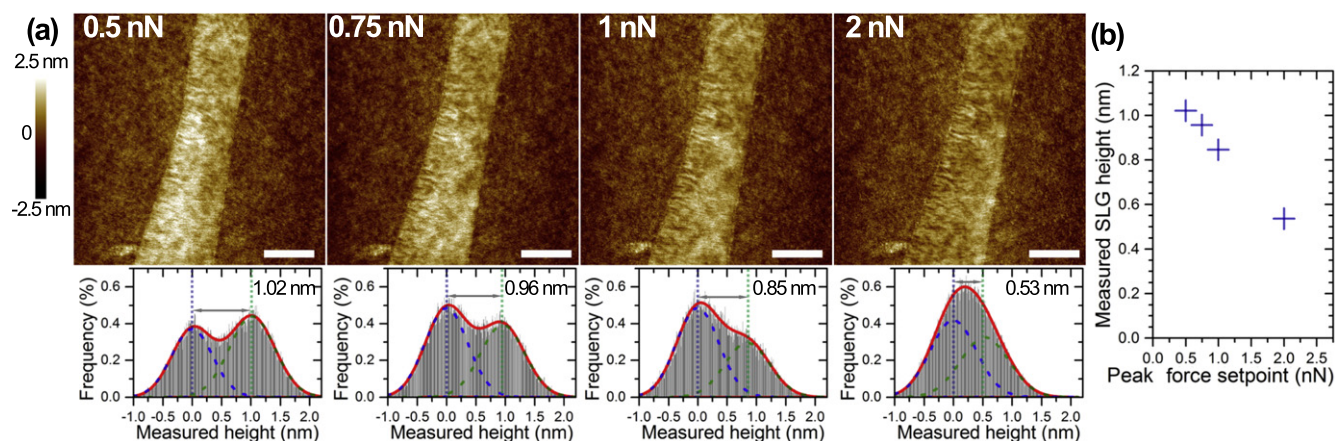


Figure 5. (a) PeakForce tapping mode AFM topography images of graphene with a SWCNT modified AFM probe showing the change in measured height with peak force set point (as indicated in each AFM image). Images were obtained sequentially for each different force set point. Below each AFM image is the corresponding histogram depth plot from which the graphene height was determined. (b) Graph of measured SLG height versus peak force set point. Scale bar = 200 nm.

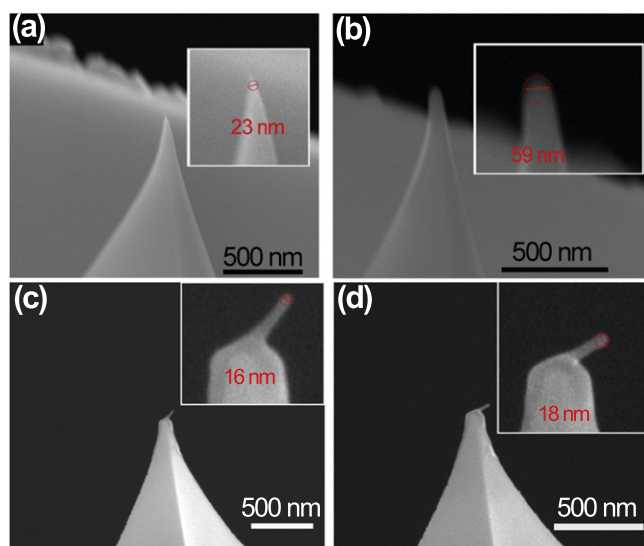


Figure 6. Representative SEM images of (a) and (b) ScanAsyst-air and (c) and (d) CNT-modified AFM probe showing the difference in tip diameter (a) and (c) before and (b) and (d) after AFM imaging with (insets) digital zoom of tip apex.

2 nN (figure 5(c)) and this trend was observed for multiple SWCNT probes (online supplementary figure S5). The key difference between standard tips and SWCNT modified probes is that the force required to measure an accurate value for graphene thickness is significantly lower (2 nN versus 10 nN). This finding supports our hypothesis that the applied pressure is the key parameter to determine accurate graphene thickness since the smaller diameter SWCNT probe will impart a higher pressure to the sample. Similar for standard AFM probes, negligible change in adhesion was observed when varying applied force (online supplementary figure S6). Imaging of MLG steps was also completed with the SWCNT probe, with insignificant change in height occurring with peak force set point and an average step height of 0.27 ± 0.04 nm obtained (online supplementary figure S7). Using such small

force for imaging would increase tip lifetime and give consistent, reliable imaging. In fact, the engage settings to begin AFM imaging were set to the lowest possible engage force. After engaging the surface, no further changes to settings were required as imaging began with ~ 2 nN peak force set point.

To confirm that the SWCNT probe has a smaller diameter than the standard tip, SEM imaging was completed on the tips both before and after use (figure 6). Tip interaction area was determined by fitting the smallest possible circle to the apex and determining the diameter. After use, the standard probe (used for the data in figure 2) was measured to have a diameter of 59 nm, which is larger than both the tip prior to imaging (23 nm, manufacturer reports a diameter range of 4–24 nm) and for the SWCNT probe (used for the data in figure 5) which showed a negligible change in diameter from 16 nm prior to use to 18 nm after use. The diameter confirms that the SWCNTs were adhered as a bundle of nanotubes. Interestingly, although the angle of the adhered SWCNT bundle changed during use, the diameter of the interaction area was not adversely affected. It is not surprising that the angle of the SWCNT bundle has changed somewhat before and after AFM measurements since it has been noted that nanotube tips often adjust to a more stable position during AFM imaging [38].

The increase in the diameter of the standard tip before and after imaging is significant and somewhat surprising as PFT applies very small forces onto the substrate when imaging. Extended scanning (up to 8 h per tip) with gradually increasing applied force beyond the standard operating force is likely to have caused the observed enhanced tip wear.

3.3. Discussion

From the findings reported herein we have assembled the following recommendations for accurate AFM imaging of graphene. If possible, prepare the samples within a moisture free environment or use hydrophobic substrates to prevent the presence of a buffer layer. If this is not feasible: use a standard

PFT probe and image with high peak force set point such that the effect of the buffer layer is negated or image with a very small diameter tip (such as a SWCNT modified probe or any probe with very small tip radius) and image with standard conditions where the pressure applied to the sample is large enough to negate the effect of the buffer layer.

When using an optimal force set point, the error related to inaccuracy of the first layer is in the order of 0.1–0.3 nm or up to one layer of graphene. Much less than the error of up to three layers for the common calculation of N in equation (1).

Although SLG is often the desired product, there are occasions where bilayer or trilayer graphene samples are prepared. It is currently not known whether imaging a bilayer graphene film with a higher applied pressure is capable of negating the error in the measured height arising from the buffer layer. We speculate that with increasing N the pressure required to accurately measure sample height will increase as pressure will dissipate through the graphene layers and not be applied onto the underlying buffer layer. Preliminary work hints that measured height of few layer graphene does decrease with applied force, however on such samples it is difficult to precisely determine N (e.g. via Raman spectroscopy) and subsequently the expected sample height. This is an area of ongoing investigation.

Unlike Raman spectroscopy, AFM does not require a specific lattice arrangement of the carbon atoms for it to obtain useful information about graphitic samples. Therefore the findings here for graphene can be applied to other graphene analogues such as graphene oxide and reduced graphene oxide as well as graphene films produced by high throughput techniques such as CVD and thermal epitaxial graphene on silicon carbide [42–44]. Furthermore, other 2D materials such as WS₂, MoS₂, MoSe₂, phosphorene and stanine would benefit from a universal, accurate and reliable method for the determination of layer number, N .

4. Conclusions

The measured height of a SLG sheet was found to vary depending upon peak force set point when using PFT AFM. By applying a large imaging force a value for height comparable to the theoretical value could be obtained. To ensure that the effect was not an imaging artefact, graphene terraces on both HOPG and a multi-layer graphite flake were imaged and the graphene terrace step height was found to remain constant, regardless of applied force. By employing a smaller diameter SWCNT-modified AFM tip the same effect of decreasing height with increasing force was observed but much lower force was required to obtain an accurate height measurement. From this finding it was hypothesized that the pressure applied to the graphene is the key parameter in accurate imaging of graphene because of the effect of an adsorbate layer between graphene and substrate. By using these findings PFT AFM can be used as an accurate and reliable method to investigate graphene samples.

Acknowledgments

The authors acknowledge the facilities of the Australian Microscopy & Microanalysis Research Facility (AMMRF) at Flinders University (AFM, Raman, SEM) and Adelaide microscopy (FIB).

References

- [1] Novoselov K S, Geim A K, Morozov S V, Jiang D, Katsnelson M I, Grigorieva I V, Dubonos S V and Firsov A A 2005 Two-dimensional gas of massless dirac fermions in graphene *Nature* **438** 197–200
- [2] Nair R R, Blake P, Grigorenko A N, Novoselov K S, Booth T J, Stauber T, Peres N M R and Geim A K 2008 Fine structure constant defines visual transparency of graphene *Science* **320** 1308
- [3] Lee C, Wei X, Kysar J W and Hone J 2008 Measurement of the elastic properties and intrinsic strength of monolayer graphene *Science* **321** 385–8
- [4] Kosuke N, Tomonori N, Koji K and Akira T 2009 Mobility variations in mono- and multi-layer graphene films *Appl. Phys. Express* **2** 025003
- [5] Zhang Y Y and Gu Y T 2013 Mechanical properties of graphene: effects of layer number, temperature and isotope *Comput. Mater. Sci.* **71** 197–200
- [6] Park H J, Meyer J, Roth S and Skákalová V 2010 Growth and properties of few-layer graphene prepared by chemical vapor deposition *Carbon* **48** 1088–94
- [7] Novoselov K S, Falko V I, Colombo L, Gellert P R, Schwab M G and Kim K 2012 A roadmap for graphene *Nature* **490** 192–200
- [8] Nilsson J, Neto A H C, Guinea F and Peres N M R 2006 Electronic properties of graphene multilayers *Phys. Rev. Lett.* **97** 266801
- [9] Casiraghi C, Hartschuh A, Lidorikis E, Qian H, Harutyunyan H, Gokus T, Novoselov K S and Ferrari A C 2007 Rayleigh imaging of graphene and graphene layers *Nano Lett.* **7** 2711–7
- [10] Ferrari A C and Basko D M 2013 Raman spectroscopy as a versatile tool for studying the properties of graphene *Nat. Nano* **8** 235–46
- [11] Ferrari A C 2007 Raman spectroscopy of graphene and graphite: disorder, electron–phonon coupling, doping and nonadiabatic effects *Solid State Commun.* **143** 47–57
- [12] Tan P H *et al* 2012 The shear mode of multilayer graphene *Nat. Mater.* **11** 294–300
- [13] Ferrari A C *et al* 2015 Science and technology roadmap for graphene, related two-dimensional crystals, and hybrid systems *Nanoscale* **7** 4598–810
- [14] Novoselov K S, Jiang D, Schedin F, Booth T J, Khotkevich V V, Morozov S V and Geim A K 2005 Two-dimensional atomic crystals *PNAS* **102** 10451–3
- [15] Shioyama H 2000 The interactions of two chemical species in the interlayer spacing of graphite *Synth. Met.* **114** 1–15
- [16] Cao P, Xu K, Varghese J O and Heath J R 2011 Atomic force microscopy characterization of room-temperature adlayers of small organic molecules through graphene templating *J. Am. Chem. Soc.* **133** 2334–7
- [17] Ochedowski O, Bussmann B K and Schleberger M 2014 Graphene on mica—intercalated water trapped for life *Sci. Rep.* **4** 6003
- [18] Mechler Á, Kokavecz J, Hesler P and Lal R 2003 Surface energy maps of nanostructures: atomic force microscopy and numerical simulation study *Appl. Phys. Lett.* **82** 3740–2

- [19] Mechler Á, Kopniczky J, Kokavecz J, Hoel A, Granqvist C-G and Heszler P 2005 Anomalies in nanostructure size measurements by afm *Phys. Rev. B* **72** 125407
- [20] Nemes-Incze P, Osváth Z, Kamarás K and Biró L P 2008 Anomalies in thickness measurements of graphene and few layer graphite crystals by tapping mode atomic force microscopy *Carbon* **46** 1435–42
- [21] Burnham N A, Behrend O P, Oulevey F, Gremaud G, Gallo P J, Gourdon D, Dupas E, Kulik A J, Pollock H M and Briggs G A D 1997 How does a tip tap? *Nanotechnology* **8** 67
- [22] Schmidt U, Dieing T, Ibach W and Hollricher O 2011 A confocal Raman-afm study of graphene *Microsc. Today* **19** 30–3
- [23] Ishigami M, Chen J H, Cullen W G, Fuhrer M S and Williams E D 2007 Atomic structure of graphene on SiO₂ *Nano Lett.* **7** 1643–8
- [24] Cao P 2011 Surface chemistry at the nanometer scale *PhD Thesis*, California Institute of Technology
- [25] Xu K, Cao P and Heath J R 2010 Graphene visualizes the first water adlayers on mica at ambient conditions *Science* **329** 1188–91
- [26] Novoselov K S, Geim A K, Morozov S V, Jiang D, Zhang Y, Dubonos S V, Grigorieva I V and Firsov A A 2004 Electric field effect in atomically thin carbon films *Science* **306** 666–9
- [27] Hosoya N, Tanimura M and Tachibana M 2013 Effect of laser irradiation on few-layer graphene in air probed by Raman spectroscopy *Trans. Mater. Res. Soc. Japan* **38** 579–83
- [28] Obraztsova E A, Osadchy A V, Obraztsova E D, Lefrant S and Yaminsky I V 2008 Statistical analysis of atomic force microscopy and Raman spectroscopy data for estimation of graphene layer numbers *Phys. Status Solidi B* **245** 2055–9
- [29] Ochedowski O, Begall G, Scheuschner N, Kharrazi M E, Maultzsch J and Schleberger M 2012 Graphene on Si(111) 7 × 7 *Nanotechnology* **23** 405708
- [30] Jung W, Park J, Yoon T, Kim T-S, Kim S and Han C-S 2014 Prevention of water permeation by strong adhesion between graphene and SiO₂ substrate *Small* **10** 1704–11
- [31] Giusca C E, Panchal V, Munz M, Wheeler V D, Nyakiti L O, Myers-Ward R L, Gaskill D K and Kazakova O 2015 Water affinity to epitaxial graphene: the impact of layer thickness *Adv. Mater. Interfaces* **2**
- [32] Eigler S, Hof F, Enzelberger-Heim M, Grimm S, Müller P and Hirsch A 2014 Statistical Raman microscopy and atomic force microscopy on heterogeneous graphene obtained after reduction of graphene oxide *J. Phys. Chem. C* **118** 7698–704
- [33] Paredes J I, Villar-Rodil S, Solís-Fernández P, Martínez-Alonso A and Tascón J M D 2009 Atomic force and scanning tunneling microscopy imaging of graphene nanosheets derived from graphite oxide *Langmuir* **25** 5957–68
- [34] Solís-Fernández P, Paredes J I, Villar-Rodil S, Martínez-Alonso A and Tascón J M D 2010 Determining the thickness of chemically modified graphenes by scanning probe microscopy *Carbon* **48** 2657–60
- [35] Jalili R, Aboutalebi S H, Esrafilzadeh D, Konstantinov K, Moulton S E, Razal J M and Wallace G G 2013 Organic solvent-based graphene oxide liquid crystals: a facile route toward the next generation of self-assembled layer-by-layer multifunctional 3D architectures *ACS Nano* **7** 3981–90
- [36] Slattery A D, Blanch A J, Quinton J S and Gibson C T 2013 Calibration of atomic force microscope cantilevers using standard and inverted static methods assisted by fib-milled spatial markers *Nanotechnology* **24** 015710
- [37] Sader J E, Sanelli J A, Adamson B D, Monty J P, Wei X, Crawford S A, Friend J R, Marusic I, Mulvaney P and Bieske E J 2012 Spring constant calibration of atomic force microscope cantilevers of arbitrary shape *Rev. Sci. Instrum.* **83** 103705
- [38] Slattery A D, Blanch A J, Quinton J S and Gibson C T 2013 Efficient attachment of carbon nanotubes to conventional and high-frequency afm probes enhanced by electron beam processes *Nanotechnology* **24** 235705
- [39] Ochedowski O, Bußmann B K and Schleberger M 2012 Laser cleaning of exfoliated graphene *MRS Proceedings* **1455** mrrs12-1455-ii08-06
- [40] Lui C H, Liu L, Mak K F, Flynn G W and Heinz T F 2009 Ultraflat graphene *Nature* **462** 339–41
- [41] Shih C-J, Strano M S and Blankschtein D 2013 Wetting translucency of graphene *Nat. Mater.* **12** 866–9
- [42] Kim H, Mattevi C, Calvo M R, Oberg J C, Artiglia L, Agnoli S, Hirjibehedin C F, Chhowalla M and Saiz E 2012 Activation energy paths for graphene nucleation and growth on Cu *ACS Nano* **6** 3614–23
- [43] Hibino H, Kageshima H, Maeda F, Nagase M, Kobayashi Y and Yamaguchi H 2008 Microscopic thickness determination of thin graphite films formed on SiC from quantized oscillation in reflectivity of low-energy electrons *Phys. Rev. B* **77** 075413
- [44] Srivastava N, Guowei H, Luxmi, Mende P C, Feenstra R M and Yugang S 2012 Graphene formed on SiC under various environments: comparison of Si-face and C-face *J. Phys. D: Appl. Phys.* **45** 154001